Environmental Science
Water Research & Technology

ROYAL SOCIETY OF CHEMISTRY

PAPER

View Article Online
View Journal | View Issue

Open Access Article. Published on 07 July 2022. Downloaded on 11/1/2025 6:51:53 PM.
This article is licensed under a Creative Commons Attribution 3.0 Unported Licence.

Check for updates

Cite this: *Environ. Sci.: Water Res. Technol.*, 2022, **8**, 2196

Environmental screening of water associated with shale gas extraction by fluorescence excitation emission matrix†

Camille Peers de Nieuwburgh, Jonathan S. Watson, Dominik J. Weiss and Mark A. Sephton *

Received 11th February 2022,
Accepted 30th June 2022

DOI: 10.1039/d2ew00112h

rsc.li/es-water

The shale revolution has involved the production of oil and gas from shale reservoirs enabled by modern techniques such as horizontal drilling and hydraulic fracturing. Large volumes of water-based fluids are required for hydraulic fracturing, some of which return to the surface as produced water. The recycling and effective disposal of produced water reduces water demand and avoids environmental impacts, respectively. Yet risks of water quality degradation surrounding shale oil and gas extraction operations remain highest during produced water treatment and disposal. Risk assessments related to produced water use are difficult to generate due to a lack of standard monitoring methods to characterise produced water and a lack of baseline monitoring data of surrounding water resources. We have performed a study on laboratory shale leachates using fluorescence excitation emission matrix (EEM) spectra and have demonstrated the utility of this spectroscopic technique as a standard method for environmental screening in which the chemical constitution of produced water is monitored. EEM spectra recorded in this work show that dissolved organic matter (DOM) in laboratory shale leachates contains chromophores such as humic acid-like and soluble microbial-like material. Short emission wavelengths (<380 nm) EEM spectra may indicate anthropogenic contamination incidents in future operations, especially as they correspond to fluorescence signatures of some injection fluid additives. Our simple fluorescence method requires little sample preparation and could be coupled with remote sensors for real time, *in situ* monitoring of contamination incidents.

Water impact

The shale revolution has been enabled by hydraulic fracturing and large volumes of water-based fluids are required which return to the surface as produced water. Here we report a study on laboratory shale leachates using fluorescence excitation emission matrix spectra and have demonstrated the utility of this spectroscopic technique as a method to monitor the chemical constitution of produced water. This simple fluorescence method requires little sample preparation and could be coupled with remote sensors for real time, *in situ* monitoring of contamination incidents.

1. Introduction

The combination of horizontal drilling techniques and high volume hydraulic fracturing has made the production of oil and gas from "unconventional" shale reservoirs possible and economically viable. Large volumes of aqueous fluid, composed of water (90.8% v:v), proppants (8.5% v:v) and a mixture of additives (0.7% v:v),[1] are injected at high pressure into a horizontal borehole to create a network of fractures in the shale. The series of vertical fractures enables hydrocarbons trapped in formations to flow back to the surface, together with water used during operations; the returning water is called "produced water". Water management during shale gas extraction operations is essential to minimise freshwater consumption while ensuring sufficient water supply for fracturing operations.[2] Water consumed for shale gas production over a 30 year life cycle can reach up to 100 million litres (L) of water per well.[3,4] Recycling and treating produced water therefore becomes an essential part of water management plans during operations.

Risks of quality degradation to surface and subsurface water in the vicinity of extraction operations is highest during disposal of non-treated water and improperly treated water, spills or leaks that occur at disposal sites, during transport to

Department of Earth Science and Engineering, Imperial College London, London, UK. E-mail: m.a.sephton@imperial.ac.uk

† Electronic supplementary information (ESI) available. See DOI: https://doi.org/10.1039/d2ew00112h

 This journal is © The Royal Society of Chemistry 2022

Open Access Article. Published on 07 July 2022. Downloaded on 11/1/2025 6:51:53 PM.
This article is licensed under a Creative Commons Attribution 3.0 Unported Licence.

disposal sites,[5–7] or *via* poor isolation of fluids due to impaired structural integrity of cement in shale gas wells.[8–10] Although contaminants in produced water are generally amenable to treatment,[11] high quantities of contaminants persist because treatment facilities are unable to detect and eliminate the array of compounds resulting from well-specific operations.[7,12] Cases of groundwater quality degradation near shale gas extraction sites have been mostly reported in studies of private drinking water wells with high concentrations of hydrocarbons such as benzene, toluene, ethylbenzene and xylene (BTEX) (from 0.2 mg L^{-1} to 7.7 mg L^{-1}), polycyclic aromatic hydrocarbons (PAHs) (averaging at 0.0054 mg L^{-1}) and diesel range organic compounds (hydrocarbons eluting between n-C_{10} and n-C_{28}) (from 0.9 mg L^{-1} to 4 mg L^{-1}) present in 95% of cases.[13–15] However, the impact of unconventional operations on surrounding water resources supply is often difficult to characterise because of the lack of monitoring of natural background levels, universality in preparation and analysis techniques, and environmental quality standards.[16] The type of monitoring and geochemical analyses performed on produced water often varies depending on the impact assessment plan, standards, and regulations implemented in the country of operations. But in nearly all monitoring scenarios, there is relatively little baseline monitoring data for water resources as extensive studies have been completed in response to perceived threats or changes mostly after operations had started.[15]

Analyses of produced water from unconventional gas extraction operations, together with fluid-rock experiments, using separation techniques, have highlighted challenges in the detection and identification of the origin of organic compounds present in produced water. Indeed, aliphatic and aromatic hydrocarbons may originate from natural shale matrices, on-site operations,[3,17] or sample storage and handling.[18,19] Anthropogenic sources of contaminants and natural signatures of water are often not distinguished. Each sedimentary basin is unique, but in all shale gas systems, methane is derived from organic matter (OM) within shales through biogenic and or thermogenic processes.[20] Dissolved organic matter (DOM) can be introduced to aquatic ecosystems during shale gas extraction operations by fracking gels (Guar gum), hydrocarbons such as BTEX, PAHs and phenols, or can be inherited from natural organic matter (NOM) present in the shale matrix (*i.e.* humic and fulvic acid).[21] Humic acid-like compounds have been reported in many wastewaters and surface waters as indigenous signatures of leaching of organic materials.[22–25]

Monitoring DOM in aquatic environments has often been used to apportion water mass sources, because each chromophore in DOM reflects the depositional environment of the organic matter.[26] However, standard methods for monitoring of DOM in waters associated with shale gas extraction operations are not currently available. Studies of the structural characteristics of DOM are complicated due to the wide range of methods used and to the complexity of inter-laboratory comparisons.[27] Characterisation of DOM usually includes extraction methods and separation techniques that prepare for analytical steps for molecular characterisation and stable isotopic measurements.[22,28] The main techniques used to characterise DOM in aquatic environments comprise UV absorbance (254 nm) and chemical oxygen demand (COD), liquid chromatography coupled with organic carbon detection (LC-OCD) or high resolution mass spectrometry (HRMS), gas chromatography–mass spectrometry (GC–MS), and Fourier transform ion cyclotron resonance–mass spectrometry (FTICR–MS).[21]

A candidate method for the standardised monitoring of DOM in waters associated with shale gas extraction is the spectroscopic technique fluorescence excitation emission matrix (EEM). EEM is increasingly being used to characterise optically active fractions of DOM, such as humic substances, and amino acids in proteins and peptides.[29,30] EEM is the sum of emission spectra of a sample at different excitation wavelengths, recorded as a matrix of fluorescent intensity in coordinates of excitation and emission wavelengths.[31] EEM spectra are repeated emission scans, collated at numerous excitation wavelengths to form 3D contour maps that permit the fractions of DOM in samples to be identified. Fluorescence spectroscopy is rapid, reagent-free, requires little sample preparation, and requires only small sample volumes in 1 or 3 ml cuvettes.

The efficiency of fluorescence EEM as a rapid and sensitive screening method to characterise DOM has been demonstrated for both fresh water[32–35] and marine ecosystems.[26,36] There are extensive reviews of the use of fluorescence EEM to characterise the dynamics of DOM in aquatic envrionments.[22,35,37] Several environmental studies have focused on the use of fluorescence EEM to trace anthropogenic inputs into natural ecosystems, such as landfill leachates,[38] oil spills[30,39] and produced water from unconventional gas extraction operations.[40,41]

There are limitations or technical bottlenecks for existing detection technologies for the environmental screening of water quality and include technical and economic challenges due to the need for real-time analyses, building contaminant specific sensors and often wireless telemetry systems.[2] Because fluorescence spectroscopy has the potential to be used in water quality studies to determine the source and origin of detected organic compounds,[41] the oil and gas industry is beginning to use fluorescent spectroscopy as a natural tracer to identify contamination incidents during operations.[30,39–42] Fluid-shale interactions are increasingly used to determine natural contributions of shale to produced water. Shale leachates are generally composed of complex mixtures of degradation products such as DOM, which include a wide range of potentially fluorescent organic compounds.[38] Due to the versatility of field measurements, sensitivity of instrumentations to a wide array of potential analytes, and the avoidance of consumable reagents and expensive sample pre-treatments, fluorescence EEM can be an ideal screening tool for *in situ* and *ex situ* analyses.[24,43]

Open Access Article. Published on 07 July 2022. Downloaded on 11/1/2025 6:51:53 PM.
This article is licensed under a Creative Commons Attribution 3.0 Unported Licence.

Such a monitoring tool may also be coupled to remote sensors[44] to provide real-time analyses, diagnostic of contamination incidences in future operations.

Yet, difficulties arise from overlapping fluorophores that create the fluorescence signature rather than individual fluorophores behaving linearly like pure components in solution.[43,45] Therefore, the identification of components based on the maximum intensity of their excitation and emission wavelengths pairs,[37] or peak picking method, enables analysis of the fluorescence EEM spectra based on emission wavelengths rather than attributing peaks to specific fluorophores.[37,46] Peaks are located in several distinct regions, each characteristic of fractions of DOM.[34] Using peak-picking, 2 distinct types of DOM fluorescent groups have been identified in aquatic ecosystems:[26] the first has fluorescence properties similar to proteins (region I and II of EEM spectra) and exhibits visually short excitation and emission wavelengths (*i.e.* excitation/emission: 200–250 nm/280–380 nm). The second has fluorescence properties similar to humic substances (region III and V of EEM spectra) with longer emission wavelengths (*i.e.* excitation/emission: 200–350 nm/380–520 nm). Fluorescence EEM in combination with peak picking analysis may therefore be used to discern the organic constitution of shale leachates and, by extrapolation, shales. Aliphatic and aromatic hydrocarbons detected in shales may be associated with humic compounds in region V[40] or with PAH-like compounds in region I.[34,47,48] Thus, fluorescence may aid characterisation of fractions of shale leachates that may not have been detected with other extraction or separation techniques such as GC–MS.

At present, challenges to monitor water quality surrounding shale gas operations fall into two categories: i) early detection of contamination incidents, and ii) efficient treatment methods to comply with discharge regulations. Environmental screening by fluorescence EEM can therefore provide a useful tool to address both of these challenges. The aim of the paper is to provide a proxy to monitor contaminant incidences in produced water in future operations, using fluorescence EEM as a screening tool. To achieve this, fluorescence signature of baseline organic compounds in laboratory shales leachates were compared with fluorescence signatures of organic compounds in hydrocarbon-contaminated seawater and produced water from the literature.

2. Materials and methods

2.1 Samples

Outcrop samples from 3 sedimentary basins in the UK were used (Table 1). All samples contained type II kerogen and were selected to include a variety of lithology, depth, total organic carbon (TOC) content, maturity (T_{max}) and hydrogen index. Access to outcrop samples with different maturities required sample collection from more than one stratigraphic level, location or basin, raising the possibility of variation in original sample constitution.

Table 1 Details of the outcrop and core samples from three basins in the UK

Sample type/lithology	Sample name	Rock Eval T_{max} (°C)	TOC (wt%)	Maturity	Basin name
Black shale	DH	434	5.56	Immature	Bowland
Black shale	AG	467	2.93	Late oil/gas window	Bowland
Edale shale	E2	439	1.16	Oil window	Edale
Blue Lias	BL	417	8.14	Immature	Wessex
Oxford clay	OC	423	8.11	Immature	Wessex
Kimmeridge clay	KC	428	10.98	Immature	Wessex
Marine shale	Y4	435	2.66	Immature	Yorkshire
Marine shale	YSS	437	0.77	Oil window	Yorkshire
Marine shale	YPS	439	0.79	Oil window	Yorkshire
Marine shale	YIS	443	0.96	Oil window	Yorkshire

2.2 Sample processing

Prior to grinding, sample surfaces were cleaned with *n*-pentane (LC–MS grade, Fisher Scientific, UK) to remove traces of contamination that may have been picked up during sample collection handling and storage. All hand specimens were crushed with a hammer, ground to a powder using a ceramic mortar and pestle, and then sieved to a particle size smaller than 125 μm to ensure sample homogeneity. Aliquots of the powders were taken for each experiment.

The leaching procedure for all experiments was as follows: 1 g of powdered sample and 10 ml of de-ionised (DI) water were transferred into a clean polytetrafluoroethylene (PTFE) test tube. Test tubes were placed on a rotary shaker for 24 hours ± 0.5; samples were then centrifuged at 1800 rpm for 20 min, and filtered through a 0.45 μm polypropylene filter (VWR, UK). Finally, the water extract of each test tube was collected in a clean glass beaker.

2.3 Excitation emission matrix measurements

Fluorescence EEM measurements were conducted using a Horiba Fluoromax-4 spectrofluorometer fitted with a Xenon excitation source. The selected method to analyse shale leachate was inspired by methods collated from the literature on OM fluorescence in several aquatic environments (Table S1 in ESI†).

Filtered leachates were transferred into a 3 ml quartz cuvette without further alterations. To obtain fluorescence EEMs, excitation wavelengths were measured from 200–500 nm with increments of 5 nm, while emission wavelengths were measured from 205–566 nm with 3 nm increments. The slit width was set to 5 nm band pass for both excitation and emission wavelength.

A water blank (18.2 MΩ cm^{-1}) was analysed at the start of each day using the same analysis technique. Instrumental drift was corrected using the Raman peak of water for each batch experiment. 3D contour plots were created by plotting fluorescence intensity as a function of emission and excitation wavelengths.[41]

 This journal is © The Royal Society of Chemistry 2022

Open Access Article. Published on 07 July 2022. Downloaded on 11/1/2025 6:51:53 PM.
This article is licensed under a Creative Commons Attribution 3.0 Unported Licence.

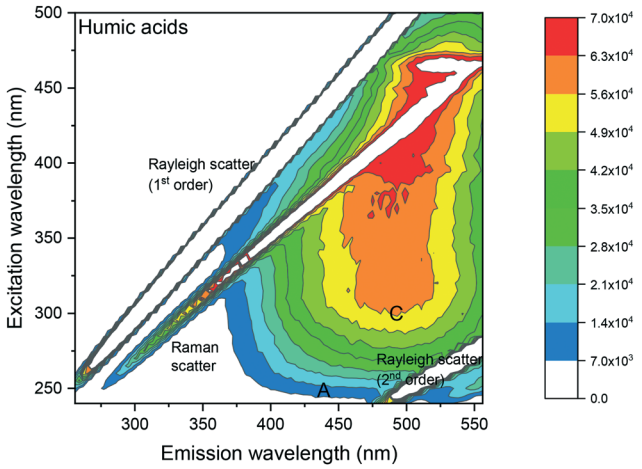

Fig. 1 Fluorescence EEM spectrum of a 1 μg mL^{-1} humic acid in DCM showing a peak at excitation/emission: 320 nm/485 nm. Fluorescence intensities (in counts per seconds (CPS)) are shown as a contour plot, with higher fluorescence intensities in red and lower fluorescence intensities in blue. Peak A: humic acid-like and fulvic acid-like material occurring in natural organic matter derived from plant material. Peak C: humic acid like material.[26,32]

A humic acid standard (Alfa Aesar, U.K.) in dichloromethane (DCM) was firstly analysed (Fig. 1), to confirm the peak maximum location in the humic acid region of the EEM spectra, thereby validating the analysis method. DCM was chosen over DI water to maximise detection of fluorescence because of the higher solubility of humic acid in DCM than in water.

3. Results

3.1 Fluorescence of humic acid

Visual analysis of the EEM spectrum of humic acid (Fig. 1) showed 2 peak maxima recorded in the humic acid-like region C at excitation/emission: 320 nm/485 nm and 460 nm/520 nm, respectively. The latter peak maximum at excitation/emission: 460 nm/520 nm, was similar to fluorescence intensities obtained in the DCM blanks (see ESI† S2). Fluorescence intensities were reported as counts per seconds (CPS) for all spectra. C denoted excitation and emission wavelengths of humic acid like-material,[26] whereas A denoted those of excitation and emission wavelength of humic acid-

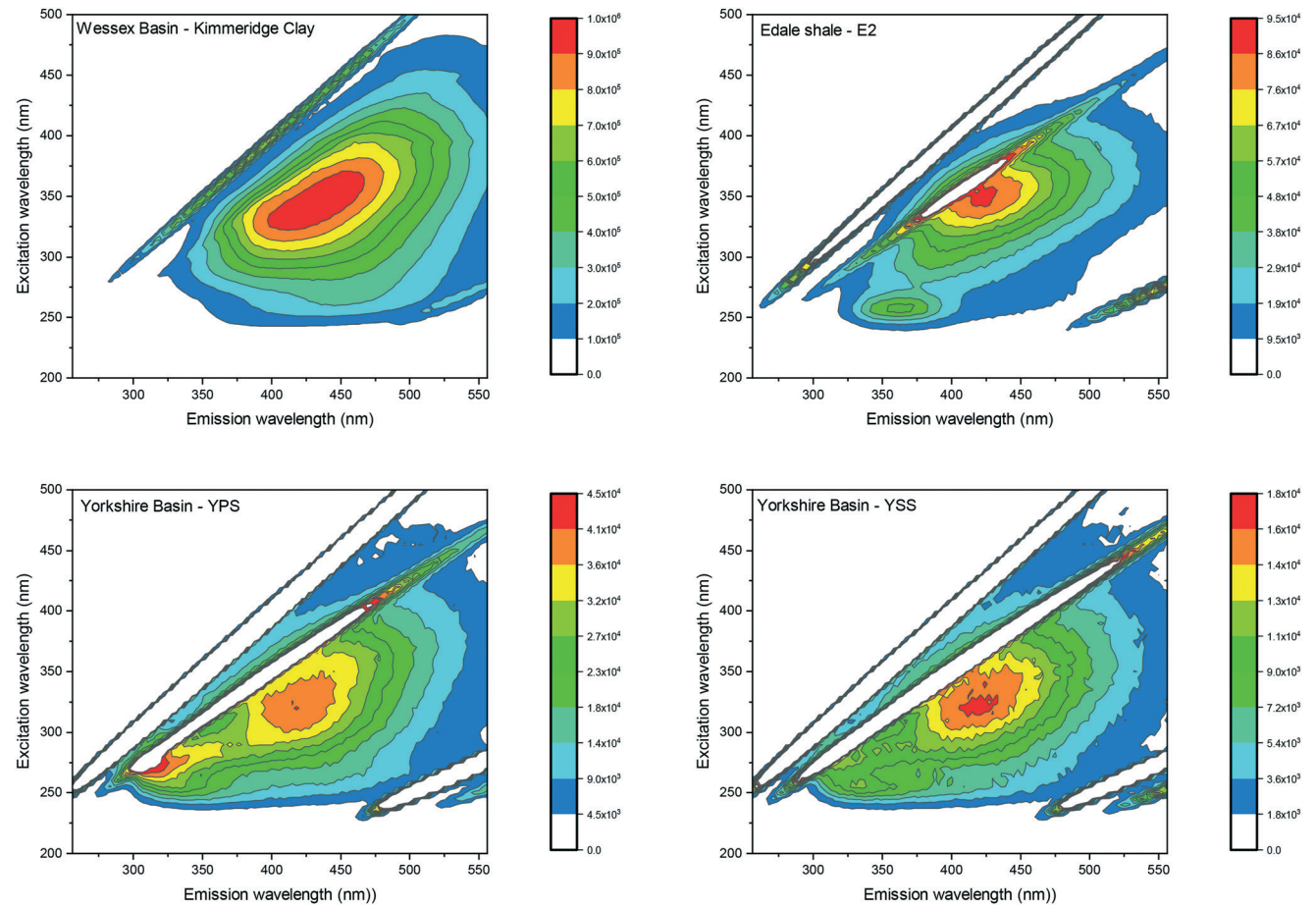

Fig. 2 EEM spectra of the Kimmeridge clay, the Edale shale sample E2 and the Yorkshire shale sample YPS and YSS. The EEM spectrum of Kimmeridge clay shows a peak maximum at excitation/emission: 350 nm/425 nm. The EEM spectra of the Edale shale sample E2, and the Yorkshire basin sample YPS and YSS, show a first primary peak at excitation/emission: 350 nm/425 nm and a secondary peak at excitation/emission: 250 nm/350 nm. All other laboratory shale leachate spectra are displayed in ESI† S3.

Open Access Article. Published on 07 July 2022. Downloaded on 11/1/2025 6:51:53 PM.
This article is licensed under a Creative Commons Attribution 3.0 Unported Licence.

like and fulvic acid-like materials[26] occurring in natural organic matter (NOM) derived from plant material.[32] The Raleigh and the water Raman light scattering were situated diagonally in the EEM spectra.

3.2 Fluorescence signature of laboratory shale leachates

Visual analyses of all laboratory shale leachates displayed single peaks located at excitations between 300 and 350 nm and emissions between 405–425 nm. Fig. 2 shows the EEM spectrum of the Kimmeridge clay as an example of the peak location recorded for all leachates. Since the analysis of EEM spectrum was visual by using the peak picking method, the results describe the location of the peak maximum only rather than fluorescence intensities. Therefore, fluorescence intensities are displayed on different scales in order to best view the peak location for each sample.

Visual analyses of sample E2 of the Edale basin and sample YPS and YSS of the Yorkshire basin displayed a secondary peak maximum, observed at short excitation and emission wavelengths (excitation/emission: 250–260 nm/305–455 nm). Fig. 2 displays the EEM spectrum for the Edale shale sample E2 as an example. The second peak appeared generally more like a shoulder than a peak with much lower intensities (averaging 50%) than the primary peaks.

3.3 Comparison with fluorescence signature of natural surface and seawater

The baseline excitation-emission peak maxima for the 3 different basins in the UK are displayed in Fig. 3 according to the 5 EEM regions and boundaries defined by Chen *et al.*[34] All primary peaks of the laboratory shale leachates were located in the region V of the EEM spectra, corresponding to humic acid-like components. The leachate peaks from the Bowland basin were located at lower excitation wavelengths than those from the other 2 basins. Secondary peak maxima were located, in the soluble microbial by-product-like region (IV). The excitation wavelength of the secondary peak of sample YSS (II) and E2 (II) is at the boundary between the soluble microbial by-product and aromatic protein II areas reflecting a relatively high influence of PAHs units.

By comparison with peak maxima of natural signatures of marine water and surface water,[34,47,48] peak maxima of sample DH, BL, Y4, YPS (I) and YSS (I) were located in the marine humic acid-like material (excitation/emission: 320/400–430 nm). Peak maximum of sample YIS, KC and OC were located in the hydrophobic acid like material (excitation/emission: 340–350/420–440 nm). Peak maxima of sample AG and E2 (I) were found in the emission spectrum of the marine humic acid like material, but at lower excitation wavelengths. All primary peaks were located at lower excitation/emission wavelengths than the humic acid-like standard. The secondary peak obtained in the soluble microbial by-product was comparable to the protein-like and phenol-like natural signature of seawater.[47,48]

3.4 Effects of maturity on the fluorescence signature of shale leachates

The organic chemical composition of shale changes with maturity as kerogen is thermally degraded to produce

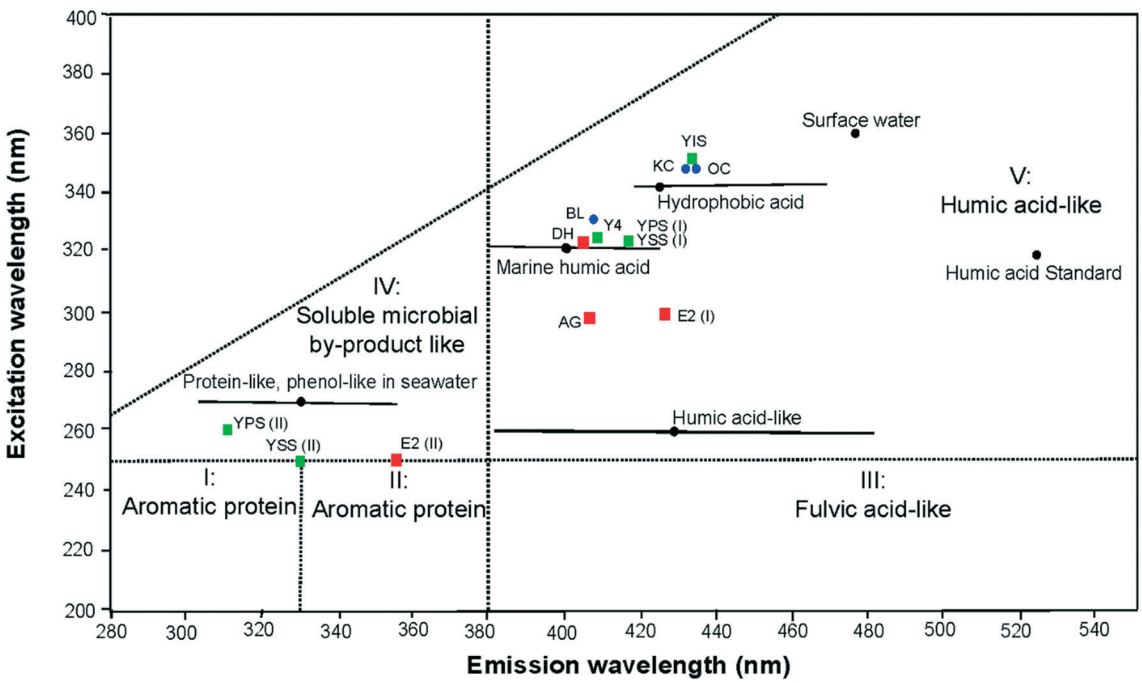

Fig. 3 Location of EEM primary peak maximum (I) in the humic acid-like region V and the secondary peak maximum (II) in the region IV. Laboratory shale leachates were colour coded depending on shale basins: Bowland basin (red square), Yorkshire basin (green square) and Wessex basin (blue dots). The peaks were compared with published signatures of natural surface water, seawater/marine water from.[34,41,47,48]

Open Access Article. Published on 07 July 2022. Downloaded on 11/1/2025 6:51:53 PM.
This article is licensed under a Creative Commons Attribution 3.0 Unported Licence.

hydrocarbons, consequently the contributions to water leachates will be partly dependent on maturity. Within the region V of the EEM spectra[34] the location of the primary peak maxima of all laboratory shale leachates reflected the maturity parameter of the shale. Leachates from high maturity shales created fluorescence signatures of shorter excitation/emission wavelengths than leachate from lower maturity shales (Fig. 4). This relationship was observed in the leachate of AG (T_{max}: 467), showing the shortest excitation/emission wavelengths of all other leachates; and the leachate OC (T_{max}: 423) showing the longest excitation/emission wavelengths of all other leachates. Uncertainties remain for the sample leachates E2, BL and YIS, which seem inconsistent with this relationship.

3.5 Fluorescence signature of produced water

Due to the very limited field measurements of produced water in the UK, fluorescence signatures of laboratory shale leachates were linked with the relatively few published fluorescence signatures of produced water (Table 2). Dahm *et al.*[41] used fluorescence signature of coalbed methane-produced water to propose a method to identify groundwater contamination incidents from gas production. The study reported a phenol-like peak (region IV) at excitation/emission: 270–280 nm/320–350 nm, 2 distinctive humic acid-like peaks (region V) at excitation/emission: 250 nm/380 nm, excitation/emission: 270 nm/400–450 nm, and one microbial by-product like peak (region IV) at excitation/emission: 300 nm/370 nm. Lester *et al.*[40] used fluorescence signature of produced water from the Niobrara shale formation of the Denver-Julesburg basin in Colorado to propose effective treatment solutions tailored for water re-use in future operations. The produced water displayed a microbial by-product like (region IV) at excitation/emission: 270 nm/300 nm and an aromatic protein like peak (region II) at excitation/emission: <250 nm/380 nm. Wang *et al.*[49] used fluorescence EEM on produced water from the Bakken shale play, the Barnett shale play and the Denver-Julesburg basin to compare produced water signature from major and newly developed oil and gas shale plays. In the study, produced water from shale oil operations in the Bakken formation displayed peaks in the region I, III and IV, associated with degraded oil-like, fulvic-acid like and microbial by-product like compounds respectively. Produced water sample from fracturing operations that employed gel based injection fluids in the Denver-Julesburg basin exhibited a microbial by-product like peak associated with the region IV of the EEM spectra.[49]

Anthropogenic fluorescence signatures of produced water usually reflect the use of additives in the injection water during operations.[50] Certain additives (*i.e.* friction reducers) also impact on the fluorescence signature of produced water with peak maxima usually flooding regions II and IV of EEM spectra;[41] while a natural signature of surface water displays a peak solely in the humic acid region V.[40]

3.6 Fluorescence signature of hydrocarbon contaminated seawater

Because of the scarcity of literature on produced water fluorescence signature and the need for fluorescence analyses of hydrocarbons in produced water, the fluorescence signature of crude oil in seawater was also related to the natural fluorescence signature of seawater (Table 2). Bianchi

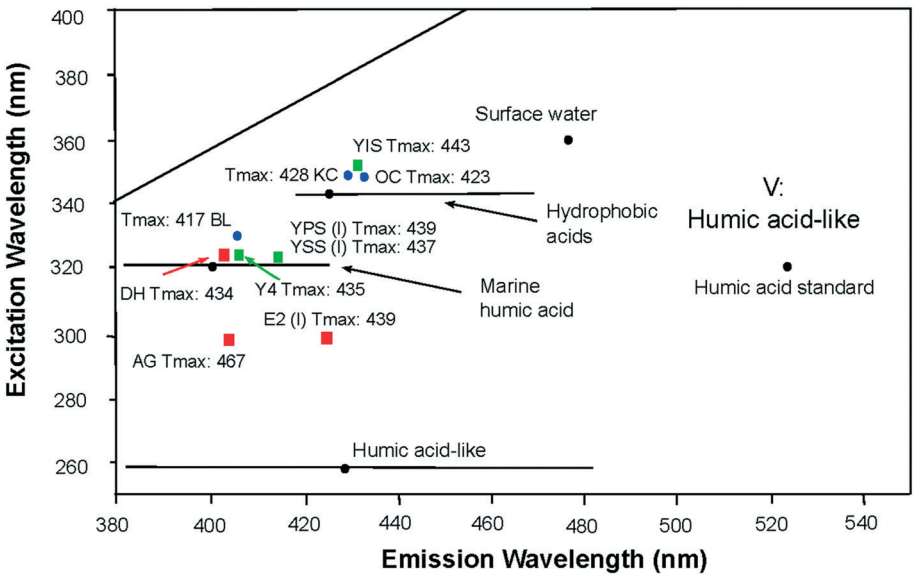

Fig. 4 Location of EEM primary peak maximum of laboratory shale leachates in the region V of the EEM spectra presented in the literature.[34,41,47,48] Maturity of shale samples are indicated as T_{max} values, under or next to the location of the peak maximum of the shale leachate leachates of high maturity shales create fluorescence signatures at shorter excitation/emission wavelengths range than leachates of lower maturity shales.

Open Access Article. Published on 07 July 2022. Downloaded on 11/1/2025 6:51:53 PM.
This article is licensed under a Creative Commons Attribution 3.0 Unported Licence.

Table 2 Fluorescence excitation emission peak maximum of produced water, surface water, additives, seawater and seawater containing crude oil from the Deepwater Horizon incident in the Gulf of Mexico that occurred in 2010. Data from conventional oil wells are included for comparison owing to the scarcity of data from shale gas wells. E_x is the excitation wavelength (nm), E_m is the emission wavelength (nm)

Samples	Letter used Parlanti *et al.* (2000)[48]	Letter used Coble *et al.* (1996)[26]	Fluorescence region Chen *et al.* (2003)[34]	E_x (max) (nm)	E_m (max) (nm)	Component type	Ref.
Seawater	α	C	V	330–350	420–480	Humic-like	48
	α'	A	V	250–260	380–480	Humic-like	
	β	M	V	310–320	380–420	Marine humic-like	
	γ	B	IV	270–280	300–320	Protein-like	
	δ	T	IV	270–280	320–350	Protein-like or phenol-like	
Seawater	α	C	V	320	440	Humic substances	47
	β	M	V	320	390	Marine humic-like	
	γ	B	IV	270	330	Protein-like/tyrosine-like	
Surface water	α	C	V	360	470	Humic acid-like	41
Produced water (Green River basin)	δ	T	IV	270–280	320–350	Phenol-like	41
	α'	A	V	250	380	Humic-like	
Produced water (Powder River basin)			IV	300	370	Microbial by-product like	
	α'	A	V	250	380	Humic-like	
Produced water (Raton basin)			V	260–270	400–450	Humic like	
Produced water (San Juan basin)	δ	T	IV	270	320	Phenol-like	
	α'	A	V	260	400–450	Humic-like	
Produced water (Denver Julesburg basin)	γ	B	IV	270	300	Microbial by-product like	40
			II	<250	380	Aromatic protein	
Produced water from oil well (Bakken basin)			I	220	290	Degraded oil-like	
	α'	A	III	240	430	Fulvic-acid like/terrestrial humic substance like	49
	γ	B	IV	270	300	Microbial by-product like	
Produced water from gel based injection fluid (Denver Julesburg basin)	γ	B	IV	270	300	Microbial by-product like	
Additives (friction reducer)			IV and II			Flooding of peaks in region II and IV	41
Gulf of Mexico crude oil			III	240	400–436	Terrestrial humic substance like	30
			I	220	290	Degraded oil-like, PAH	
			IV	255	290	Degraded oil-like, PAH	
			I	225	338	Crude oil like	
	γ	B	I	230–280	314	Amino acid-like	

et al.,[30] used fluorescence on seawater samples of the Deepwater Horizon incident in the Gulf of Mexico in 2010 and displayed degraded oil-like/crude oil like or oil-like peaks (region I) at excitation/emission: 220 nm/290–330 nm and excitation/emission: 230–280 nm/314 nm. A peak representing degraded oil-like but with higher excitation wavelengths (region IV) at excitation/emission: 255 nm/290 nm; and a terrestrial humic substance-like peak (region III) at excitation/emission: 400 nm/436 nm were observed. To compare with the fluorescence signature of natural seawater, Parlanti *et al.*[47,48] detected fluorescence spectra peaks in region IV that were interpreted as protein-like and phenol-like material (excitation/emission: 270–280 nm/300–350 nm).

4. Discussion

The visual comparison between the EEM spectra of laboratory shale leachates, natural surface water and seawater, and produced water or hydrocarbon contaminated seawater enabled us to distinguish 2 types of fluorescence signatures associated with distinctive emission wavelengths of the spectra. Emissions in the EEM spectra >380 nm correspond to region III of fulvic acid-like and region V of humic acid-like material; emissions <380 nm correspond to region I and II associated with aromatic proteins, and region IV of soluble microbial by-product like material. The 2 types of emission wavelengths detected in the spectra ultimately reflect the origins of the detected organic compounds, whether naturally occurring or as an anthropogenic addition during operations.

4.1 Detected organic compounds of natural origins: emission >380 nm

4.1.1 Fluorescence signature of laboratory shale leachates. Emissions >380 nm corresponds to humic and fulvic acid-like material, observed in surface waters and seawater. All leachates displayed a primary peak in the region of humic acid-like material (region V), around the emission wavelength of seawater samples, lower than the emissions of surface water samples. An estimated 40 to 70% of DOM[24] is composed of humic substances, which is consistent with fluorescence intensities in the region V of the EEM spectra.

 This journal is © The Royal Society of Chemistry 2022

Open Access Article. Published on 07 July 2022. Downloaded on 11/1/2025 6:51:53 PM. This article is licensed under a Creative Commons Attribution 3.0 Unported Licence.

Although humic substances in freshwater and seawater have dissimilar sources and differ chemically,[48] fluorescence of humic acid in natural water revealed 2 peaks corresponding to the letters A and C[26] or α and α'.[48] The primary peaks obtained in the humic-acid region V or the EEM spectra reflect the fluorescence studies of natural waters.

Fluorescence signatures observed in the EEM spectra are created by overlapping fluorophores rather than individual fluorophores behaving linearly like pure components in solution.[43,45] Although peak maxima observed in laboratory shale leachates are not diagnostic of individual compounds in solution, excitation wavelengths can indicate types of compounds present in the sample. High excitation wavelengths (primary peak C at 280–380 nm in all sample leachate) in region V are often associated with polycyclic fluorophores and mono-aromatic phenolic compounds.[27,37] More acidic solutions lead to peak maxima at shorter excitation wavelengths such as the secondary peak A near 250 nm observed in samples E2, YPS and YSS. Short excitation wavelengths are commonly resulting from chromophores dominated by high content of carboxylic groups. More accurate identification of individual fluorophores can be achieved using parallel factor analysis (PARAFAC) as the fluorescence signal may be separated from the underlying fluorophores mathematically.[51] Such a tool was not used in this work, as the primary focus of the study was a comparative study between fluorescence signatures rather than identifying individual fluorophores within the samples.

4.1.2 Variations in the position of peak maxima. Variations in the location of the peak maximum can be due to the pH of the leachate solution. Changes in peak positions at different pH are dependent on protonation/deprotonation of both the ground and excited states of acidic (–COOH, –OH) and basic (–NH_2) functional groups bound directly to aromatic fluorophores.[45] For example, for electron withdrawing groups, such as –COOH, protonation shifts fluorescence to longer wavelengths (red shifts) whereas deprotonation shifts the position of fluorescence to shorter wavelengths (blue shift).[40,45] This can explain the variability in the primary peak maxima of leachates between excitation: 330 nm and 340 nm and emission: 415 nm and 425 nm. Although relevant, observed changes in the fluorescence spectra owing to the effects of pH, may not be assigned to the influence of chemical structures.

Although the peak picking method is not suitable to correlate peak maximum and TOC values,[24,52] the variability in peak location within the humic acid region V seems in accordance with the maturity parameter (T_{max}) of the shale. DOM represents a heterogeneous mixture of aromatic and aliphatic organic compounds containing O, N and S functional groups.[34] Variability in shale leachate EEM spectra as a function of maturity may be anticipated.[53–55] Loss of S and O functional groups and changes in aromaticity during maturation affects the EEM signal within the humic acid region of the spectra. For example, long emission wavelengths are associated with high molecular masses components with a high degree of aromaticity.[27,56] Decrease in O and S functional groups during diagenesis are also related to decreases in concentration of humic acids in more mature samples.[57] Decrease in O and S functional groups and humic acid type response was observed for sample AG which has the highest maturity, and exhibits a fluorescence peak at shorter excitation/emissions wavelength than all other leachates. Moreover, the progressive loss of humic acid-like material in shale leachates may also be observed by comparison with the humic acid standard, exhibiting progressively lower emission wavelengths with increasing maturity, for leachates of similar pH. Given the uncertainty of this relationship for the 3 samples E2, BL and YIS, further work is needed using additional shale samples of high maturity and shale leachates of similar pH to confirm this correlation.

4.2 Detected organic compounds of anthropogenic origins: emission <380 nm

4.2.1 Fluorescence signature of produced water. Fluorescence signatures with emission <380 nm correspond to aromatic protein-like (region I and II) and soluble microbial by-product like or phenol-like compounds (region IV). As expected, primary peaks in the laboratory shale leachates were absent from the region II of the EEM spectra, which is associated with anthropogenic activities in wastewater studies.[37,58] Well additives used in unconventional gas operations (*e.g.* friction reducers) have distinctive geochemical signatures,[40,50] and generally display fluorescence intensities in region II of EEM spectra.[41] In this region, fluorophores contain a limited number of aromatic rings,[37] such as crude oil-derived compound,[30,39] or PAH-like compounds.[51] The absence of peaks at short emission wavelengths (<380 nm) in natural freshwater, seawater, and laboratory shale leachates implies that short emission wavelengths associated with short excitation wavelengths (*i.e.* region II) could be used as a proxy to determine contamination incidents during produced water quality monitoring. Indeed, water impacted by hydrocarbons were previously assigned to fluorescence signatures characterised by blue-shifted intensities (*i.e.* <380 nm).[40,49] Contrasting results from laboratory shale leachates and produced water, demonstrates the clear fingerprint of compounds arising from different origins compared with anthropogenic activities.

4.2.2 Discrimination between sources using peak picking. At short emission wavelengths, peaks corresponding to the letters T and B[26] or δ and γ (ref. 48) were also detected in laboratory shale leachates (secondary peaks in samples E2, YPS and YSS), seawater,[47] produced water from coalbed methane,[41] and produced water from the Niobrara shale gas extraction operations that employs slickwater as injection fluid[40] or gel based injection fluid.[49] While the peaks in natural seawater were strongly associated with microbial activities,[26,27,39,47,48] fluorophores in produced water, within

Open Access Article. Published on 07 July 2022. Downloaded on 11/1/2025 6:51:53 PM.
This article is licensed under a Creative Commons Attribution 3.0 Unported Licence.

the same region of the EEM spectra were associated with phenolic compounds.[30,37,40,41]

The presence of short emission peaks in the region IV of the EEM spectra is also naturally present in seawater samples.[33,47] Since shales are formed in marine environments, organic matter present in shale must therefore reflect the composition of seawater column during deposition. Peaks observed in shale leachates at short emission wavelengths are therefore concluded to be of natural origin.

In produced water, although peaks in region IV of EEM spectra may be attributed to phenol-like components, their origin may still be natural rather than anthropogenic. Indeed, the composition of produced water is known to reflect not only the injection water, but also the formation water entrapped in the shale.[9] High salinity is often recorded in produced water samples.[50,59,60] Although the origin of salinity remains under debate, there is a consensus that the dissolution of salts and diffusion of ions present within shales during their formation in open marine environment contributes up to 80% of the composition of produced water.[61,62] In this case, mobilisation of ions and salt minerals from formation water to produced water contributes to the overall fluorescence signature of produced water in region IV of the EEM spectra. Comparison between fluorescence spectra of laboratory shale leachates and produced water in the literature[40,41,49] imply that the composition of shales directly impacts the overall fluorescence signatures of the EEM spectra in both shale leachates and produced water. Nevertheless, discrimination between sources using fluorescence spectroscopy and region IV of the EEM spectra remains challenging since produced water may still reflect the signature of injected fluid and additives as well as formation water.

4.3 EEM spectra for the monitoring of produced water

Monitoring wells during operations can warrant careful water management plans during operations, enable better informed treatment decisions or the design of mitigation plans, as well as helping to implement immediate effective remedial actions in the case of contamination incidents. Challenges still remain when monitoring contamination incidences in water resources surrounding shale gas extraction operations. First, monitoring needs to be site-specific and well-specific and a full appreciation of compounds that may enter water resources needs to be adequately characterised. While the design of injection fluids is often tailored to suite the geochemical and geophysical properties of the shale formation in each well, building contaminant specific-sensors still remains a technical and economic challenge.[2] Second, monitoring contaminant incidences often requires real-time analyses and often wireless telemetry systems.[2,24] To date, many chemical, physical and microbiological tests to assess wastewater quality are unsuitable for real-time monitoring.[37] Beyond on-site implications, the connection between water and energy is multifaceted and includes facilities maintenance, longevity of equipment, weatherproofing, and other physical site considerations. The so-called water-energy nexus is dealt with comprehensively in the literature.[63]

Real-time monitoring of water quality during operations offers the opportunity to bridge the gap between monitoring water quality as a response to an existing threat and obtaining information on the quality of water prior to extraction operations. Due to the versatility of field measurements, sensitivity of instrumentation to a wide array of potential analytes, and the avoidance of consumable reagents and expensive sample pre-treatments, fluorescence EEM may be used as real-time monitoring tool for *in situ* and *ex situ* analyses.[24,43] Fluorescence spectroscopy using EEM was demonstrated as a simple tool to analyse water and monitor its quality: data collection requires little sample preparation and could be coupled with remote sensors for the real time *in situ* monitoring of incidents.

The suitability to accurately monitoring water surrounding unconventional gas operations using fluorescence EEM lies in the use of the detection of peaks in the region II of the EEM spectra as a proxy for detecting anthropogenic activities. The lack of selectivity in fluorescence spectroscopy may still create challenges in determining and discriminating the source of fluorescence intensities, especially for interpreting peaks in the region IV of the EEM spectra. Challenges may still remain when using the peak picking method because the pH of injection fluids and salinity of recovered produced water may affect the chromophoric DOM composition of samples, thereby altering the signatures of the EEM spectra.

5. Conclusion

This study effectively observed fluorescence signatures of laboratory shale leachates and compared them with fluorescence signatures of produced water and hydrocarbon contaminated seawater obtained in the literature. The consistency in the EEM spectra recorded in this work clearly shows that DOM in laboratory shale leachates contains chromophores such as humic acid-like and soluble microbial-like material. Fluorescence spectra of laboratory shale leachates exhibited similarities to the fluorescence signatures of natural fresh- and marine water, although quite different from those of produced water and hydrocarbon contaminated seawater with peaks at shorter emission wavelengths of emission <380 nm. Peaks in the region II of the EEM spectra were consistently attributed to anthropogenic activities. Therefore, short emission wavelengths (<380 nm) in region II of EEM spectra may indicate anthropogenic contamination incidents in future operations, especially as they correspond to fluorescence signatures of some injection fluid additives. The lack of selectivity in fluorescence spectroscopy may still create challenges in determining and discriminating the source

 This journal is © The Royal Society of Chemistry 2022

Open Access Article. Published on 07 July 2022. Downloaded on 11/1/2025 6:51:53 PM.
This article is licensed under a Creative Commons Attribution 3.0 Unported Licence.

fluorescence intensities occurring in the region IV of the EEM spectra.

Operators would benefit from the use of environmental screening by fluorescence EEM as immediate remedial actions could be taken in the case of contamination incidents by anthropogenic sources. Fluorescence EEM is a simple method to analyse water and to monitor water quality in the vicinity of shale gas operations; data collection requires little sample preparation and could be coupled with remote sensors for the real time, *in situ* monitoring of incidents. Real-time fluorescence monitoring offers an opportunity to bridge the gap between monitoring water quality in response to an existing threat, and obtaining information on water quality prior to extraction operations.

Conflicts of interest

There are no conflicts of interest to declare.

References

1 A. Aminto and M. S. Olson, *J. Nat. Gas Sci. Eng.*, 2012, **7**, 16–21.
2 J.-H. Son, A. Hanif, A. Dhanasekar and K. H. Carlson, *Environ. Monit. Assess.*, 2018, **190**, 138.
3 D. Costa, J. Jesus, D. Branco, A. Danko and A. Fiúza, *Environ. Sci. Pollut. Res.*, 2017, **24**, 14579–14594.
4 H. Chen and K. E. Carter, *J. Environ. Manage.*, 2016, **170**, 152–159.
5 T. L. S. Silva, S. Morales-Torres, S. Castro-Silva, J. L. Figueiredo and A. M. T. Silva, *J. Environ. Manage.*, 2017, **200**, 511–529.
6 K. B. Gregory, R. D. Vidic and D. A. Dzombak, *Elements*, 2011, **7**, 181–186.
7 S. Adham, A. Hussain, J. Minier-Matar, A. Janson and R. Sharma, *Desalination*, 2018, **440**, 2–17.
8 S. B. C. Shonkoff, J. Hays and M. L. Finkel, *Environ. Health Perspect.*, 2014, **122**, 787–795.
9 A. Vengosh, R. B. Jackson, N. Warner, T. H. Darrah and A. Kondash, *Environ. Sci. Technol.*, 2014, **48**, 8334–8348.
10 R. Lefebvre, *Wiley Interdiscip. Rev.: Water*, 2017, **4**, e1188.
11 M. K. Camarillo, J. K. Domen and W. T. Stringfellow, *J. Environ. Manage.*, 2016, **183**, 164–174.
12 L. He, Y. Chen, H. Zhao, P. Tian, Y. Xue and L. Chen, *Sci. Total Environ.*, 2018, **627**, 1585–1601.
13 D. C. DiGiulio and R. B. Jackson, *Environ. Sci. Technol.*, 2016, **50**, 4524–4536.
14 E. A. Chittick and T. Srebotnjak, *J. Environ. Manage.*, 2017, **204**, 502–509.
15 J. L. Luek and M. Gonsior, *Water Res.*, 2017, **123**, 536–548.
16 I. Vandecasteele, I. M. Rivero, S. Sala, C. Baranzelli, R. Barranco, O. Batelaan and C. Lavalle, *Environ. Manage.*, 2015, **55**, 1285–1299.
17 A. Butkovskyi, H. Bruning, S. A. E. Kools, H. H. M. Rijnaarts and A. P. Van Wezel, *Environ. Sci. Technol.*, 2017, **51**, 4740–4754.
18 J. J. Brocks, E. Grosjean and G. A. Logan, *Geochim. Cosmochim. Acta*, 2008, **72**, 871–888.
19 E. Grosjean and G. A. Logan, *Org. Geochem.*, 2007, **38**, 853–869.
20 T. Zhang, G. S. Ellis, S. C. Ruppel, K. Milliken and R. Yang, *Org. Geochem.*, 2012, **47**, 120–131.
21 S. M. Riley, D. C. Ahoor, J. Regnery and T. Y. Cath, *Sci. Total Environ.*, 2018, **613–614**, 208–217.
22 J. B. Fellman, E. Hood and R. G. M. Spencer, *Limnol. Oceanogr.*, 2010, **55**, 2452–2462.
23 C. Manzano, E. Hoh and S. L. M. Simonich, *J. Chromatogr. A*, 2013, **1307**, 172–179.
24 E. M. Carstea, A. Baker, M. Bieroza and D. Reynolds, *Water Res.*, 2010, **44**, 5356–5366.
25 P. Giamarchi, L. Stephan, S. Salomon and A. Le Bihan, *J. Fluoresc.*, 2000, **10**, 393–402.
26 P. G. Coble, *Mar. Chem.*, 1996, **51**, 325–346.
27 M. M. D. Sierra, M. Giovanela, E. Parlanti and E. J. Soriano-Sierra, *Chemosphere*, 2005, **58**, 715–733.
28 R. G. M. Spencer, G. Aiken, K. P. Wickland, R. Striegl and P. J. Hernes, *Global Biogeochem. Cycles*, 2008, **22**, GB4002.
29 N. Hudson, A. Baker and D. Reynolds, *River Res. Appl.*, 2007, **23**, 631–649.
30 T. S. Bianchi, C. Osburn, M. R. Shields, S. Yvon-Lewis, J. Young, L. Guo and Z. Zhou, *Environ. Sci. Technol.*, 2014, **48**, 9288–9297.
31 K. Bengraïne and T. F. Marhaba, *J. Hazard. Mater.*, 2004, **108**, 207–211.
32 A. Baker, *Environ. Sci. Technol.*, 2001, **35**, 948–953.
33 A. Baker and R. G. M. Spencer, *Sci. Total Environ.*, 2004, **333**, 217–232.
34 W. Chen, P. Westerhoff, J. A. Leenheer and K. Booksh, *Environ. Sci. Technol.*, 2003, **37**, 5701–5710.
35 R. K. Henderson, A. Baker, K. R. Murphy, A. Hambly, R. M. Stuetz and S. J. Khan, *Water Res.*, 2009, **43**, 863–881.
36 R. Del Vecchio and N. V. Blough, *Mar. Chem.*, 2002, **78**, 231–253.
37 E. M. Carstea, J. Bridgeman, A. Baker and D. M. Reynolds, *Water Res.*, 2016, **95**, 205–219.
38 A. Baker and M. Curry, *Water Res.*, 2004, **38**, 2605–2613.
39 Z. Zhou, L. Guo, A. M. Shiller, S. E. Lohrenz, V. L. Asper and C. L. Osburn, *Mar. Chem.*, 2013, **148**, 10–21.
40 Y. Lester, I. Ferrer, E. M. Thurman, K. A. Sitterley, J. A. Korak, G. Aiken and K. G. Linden, *Sci. Total Environ.*, 2015, **512–513**, 637–644.
41 K. G. Dahm, C. M. Van Straaten, J. Munakata-Marr and J. E. Drewes, *Environ. Sci. Technol.*, 2013, **47**, 649–656.
42 G. Ferrari and M. Mingazzini, *Mar. Ecol.: Prog. Ser.*, 1995, **125**, 305–315.
43 R. D. JiJi, G. A. Cooper and K. S. Booksh, *Anal. Chim. Acta*, 1999, **397**, 61–72.
44 J. H. Goldman, S. A. Rounds and J. A. Needoba, *Environ. Sci. Technol.*, 2012, **46**, 4374–4381.
45 *Aquatic Organic Matter Fluorescence*, ed. P. G. Coble, J. Lead, A. Baker, D. M. Reynolds and R. G. M. Spencer, Cambridge University Press, Cambridge, 2014.

Open Access Article. Published on 07 July 2022. Downloaded on 11/1/2025 6:51:53 PM.
This article is licensed under a Creative Commons Attribution 3.0 Unported Licence.

46 W.-T. Li, S.-Y. Chen, Z.-X. Xu, Y. Li, C.-D. Shuang and A.-M. Li, *Environ. Sci. Technol.*, 2014, **48**, 2603–2609.
47 E. Parlanti, B. Morin and L. Vacher, *Org. Geochem.*, 2002, **33**, 221–236.
48 E. Parlanti, K. Wörz, L. Geoffroy and M. Lamotte, *Org. Geochem.*, 2000, **31**, 1765–1781.
49 H. Wang, L. Lu, X. Chen, Y. Bian and Z. J. Ren, *Water Res.*, 2019, **164**, 114942.
50 W. Orem, C. Tatu, M. Varonka, H. Lerch, A. Bates, M. Engle, L. Crosby and J. McIntosh, *Int. J. Coal Geol.*, 2014, **126**, 20–31.
51 L. Yang, D. H. Han, B.-M. Lee and J. Hur, *Chemosphere*, 2015, **127**, 222–228.
52 J. H. Weber and S. A. Wilson, *Water Res.*, 1975, **9**, 1079–1084.
53 G. Hattori, J. Trevelyan, C. E. Augarde, W. M. Coombs and A. C. Aplin, *Arch. Comput. Methods Eng.*, 2017, **24**, 281–317.
54 P. R. Craddock, T. V. Le Doan, K. Bake, M. Polyakov, A. M. Charsky and A. E. Pomerantz, *Energy Fuels*, 2015, **29**, 2197–2210.
55 M. Radke, *Mar. Pet. Geol.*, 1988, **5**, 224–236.
56 N. Her, G. Amy, D. McKnight, J. Sohn and Y. Yoon, *Water Res.*, 2003, **37**, 4295–4303.
57 A. Y. Huc and B. M. Durand, *Fuel*, 1977, **56**, 73–80.
58 H. Yu, Y. Song, R. Liu, H. Pan, L. Xiang and F. Qian, *Chemosphere*, 2014, **113**, 79–86.
59 Y. Hu, D. Devegowda, A. Striolo, A. Phan, T. A. Ho, F. Civan and R. Sigal, *J. Unconv. Oil Gas Resour.*, 2015, **9**, 31–39.
60 I. Ferrer and E. M. Thurman, *Trends Environ. Anal. Chem.*, 2015, **5**, 18–25.
61 N. R. Warner, R. B. Jackson, T. H. Darrah, S. G. Osborn, A. Down, K. Zhao, A. White and A. Vengosh, *Proc. Natl. Acad. Sci. U. S. A.*, 2012, **109**, 11961.
62 N. R. Warner, T. H. Darrah, R. B. Jackson, R. Millot, W. Kloppmann and A. Vengosh, *Environ. Sci. Technol.*, 2014, **48**, 12552–12560.
63 G. Olssen, *Water and Energy: Threats and Opportunities, IWA Publishing*, 2nd edn, 2015, vol. 14.

 This journal is © The Royal Society of Chemistry 2022